

Title	Weldability of Fe-36%Ni Alloy (Report V) : Behaviors of Grain-boundary Sliding and Cavity Formation Preceding Reheat Hot Cracking in Weld Metal(Materials, Metallurgy & Weldability)
Author(s)	Zhang, Yue-Chang; Nakagawa, Hiroji; Matsuda, Fukuhisa
Citation	Transactions of JWRI. 1985, 14(2), p. 319-324
Version Type	VoR
URL	<a href="https://doi.org/10.18910/6563">https://doi.org/10.18910/6563</a>
rights	
Note	

***Osaka University Knowledge Archive : OUKA***

<https://ir.library.osaka-u.ac.jp/>

Osaka University

# Weldability of Fe-36%Ni Alloy (Report V)<sup>†</sup>

— Behaviors of Grain-boundary Sliding and Cavity Formation Preceding Reheat Hot Cracking in Weld Metal —

Yue-Chang ZHANG\*, Hiroji NAKAGAWA\*\* and Fukuhisa MATSUDA\*\*\*

## Abstract

To reveal the mechanism of reheat hot cracking in weld metal of Invar, microstructural behaviors concerning the cracking, namely grain-boundary sliding, cavity formation, grain-boundary migration and recrystallization during hot ductility test were studied. Main conclusions obtained are as follows: (1) Grain-boundary sliding and its resultant cavity formation are prerequisite to the cracking. (2) One of the reason for high ductility in the temperature below the temperature region giving ductility trough causing the crack is the difficulty of grain-boundary sliding. (3) Grain-boundary migration and dynamic recrystallization have important roles in raising the ductility in the high temperature region of the ductility trough.

**KEY WORDS:** (Hot Cracking) (Controlled Expansion Alloys) (Containers) (GTA Welding)

## 1. Introduction

The dynamic observation of the reheat hot cracking in the weld metal of Fe-36%Ni alloy Invar by means of hot stage microscope in the previous paper<sup>1)</sup> revealed that grain-boundary sliding and its resultant cavity formation are prerequisite to the cracking. The heating rate by hot stage microscope, however, was very slow and thus fairly different from that in actual welding. Also its constant loading mode during the dynamic observation is considered to be different from actual welding. Therefore, it is necessary to confirm whether grain-boundary sliding and cavity formation are concerned with the cracking in actual welding.

On the other hand, the authors confirmed<sup>2)</sup> that the ductility trough connecting with the reheat hot cracking can be simulated well by means of simulated hot ductility test with rapid heating rate under proper crosshead speed. Therefore in this study, the grain-boundary sliding, the cavity formation and its coalescence, and other microstructural phenomena occurring during the hot ductility test were studied mainly. Finally, it was checked a little whether they are concerned in actual cracking test.

## 2. Materials Used and Experimental Procedures

### 2.1 Materials used

The chemical compositions of four tentative Fe-36%Ni alloys used are shown in Table 1, where the Items follow those in the Report II<sup>3)</sup> and L means the total crack length<sup>3)</sup> in the Cross-bead tensile hot cracking test under 150 MPa. It is understood that the materials of high and low crack susceptibilities were prepared. Their thickness was 3 mm except 1.5 mm of Item Nos. 10 and 13.

Table 1 Chemical compositions of materials used.

Item No.	Chemical composition (wt.%)								
	C	Si	Mn	P	S	N	O	Al*	Ni
1	0.031	0.20	0.50	0.002	0.0011	0.0008	0.0034	0.009	36.25
10	0.032	0.20	0.36	0.001	0.008	0.0011	0.0018	0.001	36.24
12	0.033	0.19	0.35	0.003	0.005	0.0035	0.0021	0.001	36.05
13	0.028	0.19	0.35	0.004	0.004	0.0047	0.0038	0.001	34.97

\*: soluble

### 2.2 Simulated hot ductility test

The configuration of the specimen used in the simulated hot ductility test is shown in Fig. 1, where weld metal was located in the middle of the specimen. The welding was done with GTAW (DCEN) under the conditions of welding current of 100–105A, arc voltage of 11–13V and

<sup>†</sup> Received on Oct. 30, 1985

\* Foreign Researcher (Shanghai Jiao Tong Univ.)

\*\* Research Instructor

\*\*\* Professor

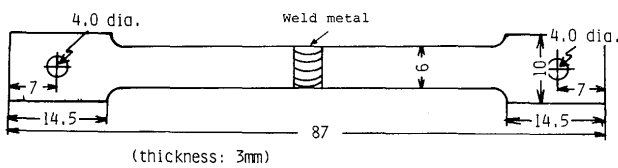


Fig. 1 Specimen configuration used for simulated hot ductility test.

welding speed of 100 mm/min with Ar back shielding. The bead width of top and back surfaces was about 5–6 mm. The test was done with high frequency induction heating system in Ar atmosphere, and its heating and loading programs are shown in Fig. 2. Three kinds of crosshead speed, namely  $\dot{d}_h$  (13.3 mm/sec),  $\dot{d}_m$  (0.56 mm/sec) and  $\dot{d}_l$  (0.093 mm/sec) were used. Strain rate  $\dot{\epsilon}$  evaluated at 900°C by the gage length of 5 mm in the weld metal was about 0.75/sec under  $\dot{d}_h$ , about 0.03/sec under  $\dot{d}_m$  and about 0.003/sec under  $\dot{d}_l$ . Ductility was evaluated by the ratio of reduction of the specimen width after the testing to the original width, and is represented as  $\Delta W/W \times 100(\%)$ , where  $\Delta W$  is the reduction of the width and  $W$  is the original width.

The surface of specimen was polished electrolytically, and straight marking lines to measure grain-boundary sliding were drawn on the surface of weld metal by a razor. The displacement of grain-boundary sliding along the loading direction was measured by optical microscope in  $\times 400$ . The number of measurement per one specimen was about thirty. The degree of grain-boundary migration was evaluated on the surface by optical microscope in the following manner: Since generally one grain-boundary did not necessarily migrate at its overall parts, the number of grain-boundaries which migrated even a little in one field of microscope in  $\times 200$  was counted, and the total of such grain-boundaries were named  $N_{mgb}$ . The total of grain-boundaries observed in weld metal,  $N_{gb}$ , was about 300. Now the ratio of grain-boundary migration was defined as  $N_{mgb}/N_{gb} \times 100(\%)$ . Then, the degree of dynamic recrystallization was evaluated by the fraction of recrystallization area,  $f_R$ , which was measured on the

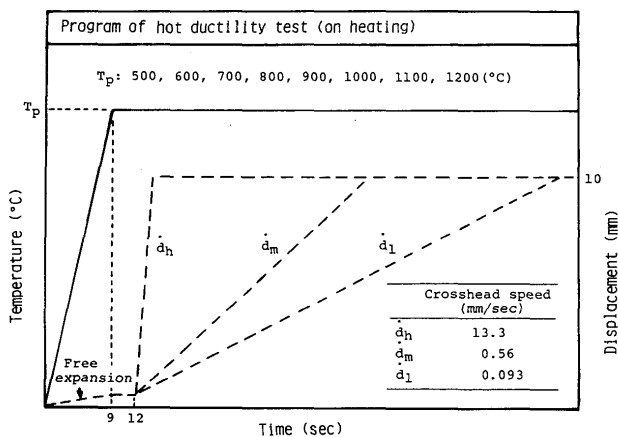


Fig. 2 Program of simulated hot ductility test.

surface by point counting method in  $\times 200$ . The number of fields measured was about 60.

### 2.3 Weld hot cracking test

In order to check roughly whether the microstructural behaviors observed in the simulated hot ductility test are concerned in actual weld cracking, the surface of weld metal and the cracked surface after the Cross-bead cracking test and the Parallel-bead cracking test utilizing the U-form hot cracking device<sup>4)</sup> for Item Nos. 10 and 13 were observed by SEM. Both the first and the second pass welding was done with GTAW without filler metal under the following conditions; welding current of 60A, arc voltage of 9–11V and welding speed of 100 mm/min. The Cross-bead cracking test was done in a welding chamber filled with 99.99% Ar gas after evacuation to  $5 \times 10^{-5}$  torr. in order to prevent the oxidation of surface of weld metal.

## 3. Experimental Results and Discussions

### 3.1 Behavior of grain-boundary sliding

Typical examples of microscopic deformation mode in Item No. 12 at 600, 900 and 1100°C under  $\dot{d}_m$  are shown in Fig. 3. There is little grain-boundary sliding but are many slip bands within grains at 600°C where the hot ductility has a clear high value which recovers fairly from the low level at about 900°C. On the other hand, at 900°C corresponding nearly to the minimum ductility temperature and at 1100°C, grain-boundary sliding is clearly seen and slip bands are relatively indistinct.

The distribution of the displacement of grain-boundary sliding along loading direction at 600, 900 and 1100°C is shown in Fig. 4. Based on this distribution, average displacement of grain-boundary sliding per one grain-boundary at  $\epsilon=1$  where  $\epsilon$  means total strain of weld metal, namely  $\bar{S}_{gb/\epsilon=1}$ , is shown in Fig. 5. It is seen that  $\bar{S}_{gb/\epsilon=1}$  is very small at 600°C and increases toward 900°C, and then decreases again. As mentioned later in detail, the reason why  $\bar{S}_{gb/\epsilon=1}$  at 1100°C is smaller than that at 900°C is that the grain-boundary sliding is suppressed by active grain-boundary migration and dynamic recrystallization at 1100°C. Because the hot ductility has a tendency to recover above 1100°C and below 600°C as shown in the previous paper<sup>2)</sup>, it is understood that grain-boundary sliding is prerequisite to the ductility trough causing the reheat hot cracking.

The hot ductility test in the previous paper<sup>2)</sup> showed that the increase in crosshead speed raises the ductility. Concerning this, Fig. 6 shows the deformation mode at 900°C under  $\dot{d}_h$ , and it is seen that there is hardly grain-boundary sliding but many slip bands comparing Fig. 3(b). Figure 7 shows the dependency of  $\bar{S}_{gb/\epsilon=1}$  on strain rate at 900°C, and means clearly that high strain rate suppresses the grain-boundary sliding. This is the reason why

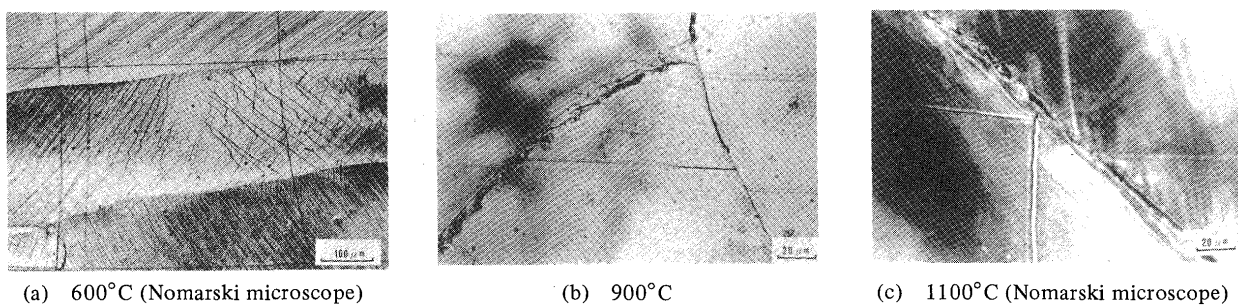
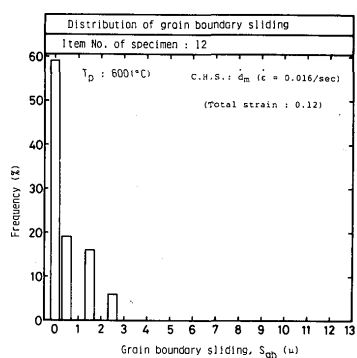
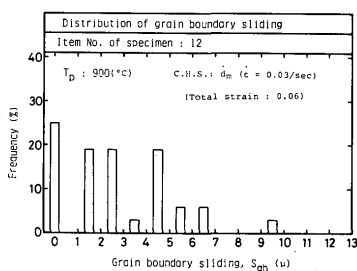


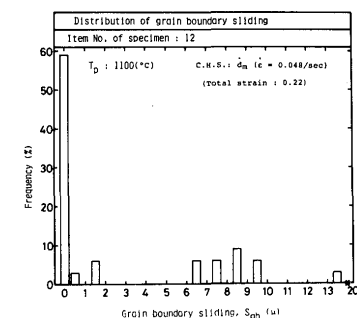
Fig. 3 Microscopic deformation mode at different testing temperature under crosshead speed (C.H.S.) of  $\bar{d}_m$ , Item No. 12.



(a) 600°C



(b) 900°C



(c) 1100°C

Fig. 4 Frequency distribution of displacement of grain-boundary sliding under C.H.S. of  $\bar{d}_m$ .

the hot ductility is raised with the increase in crosshead speed.

### 3.2 Formation and coalescence of cavities

As the result of grain-boundary sliding, cavities were formed and coalesced. One of the examples is shown in Fig. 8(a), and it seems that cavities were formed at ledges of grain-boundary, which will be discussed in detail concerning grain-boundary serration in the next paper<sup>5</sup>). An

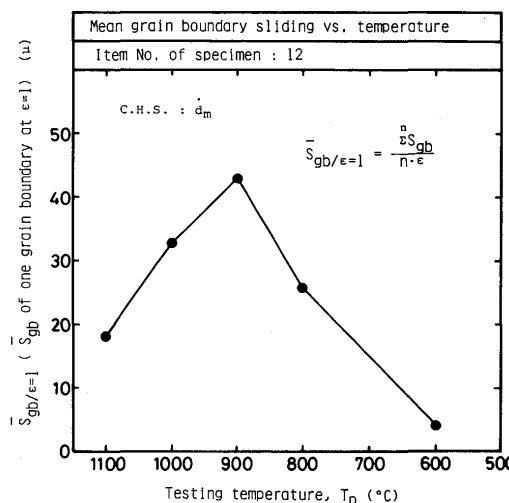


Fig. 5 Relation between temperature and average displacement of grain-boundary sliding per one grain-boundary at  $\epsilon = 1$  where  $\epsilon$  means the strain in weld metal, C.H.S. :  $\bar{d}_m$ .

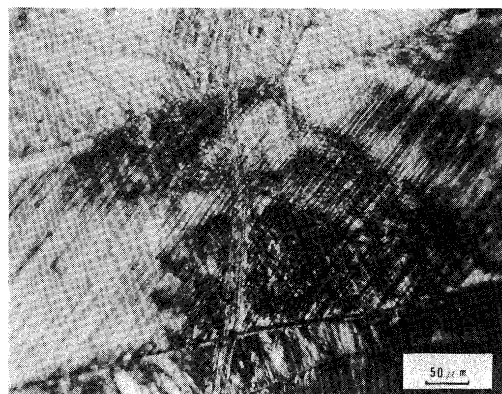


Fig. 6 Microscopic deformation mode under high crosshead speed  $\bar{d}_h$  at 900°C, Item No. 12.

example of surface cracking by the coalescence of cavities is shown in Fig. 8(b) together with cracked surface peeping out. The cracked surface has a feature of wavy pattern as seen in the previous paper<sup>1</sup>). It may be supposed that this wavy or rounded feature of the cracked surface was caused by local liquation of grain-boundary, because Fe-36%Ni alloy has a possibility to form  $\text{Ni}_3\text{S}_2$  type sulphides whose eutectic temperature with Ni is 645°C. As shown in the next paper<sup>5</sup>), however, any nickel sulphide

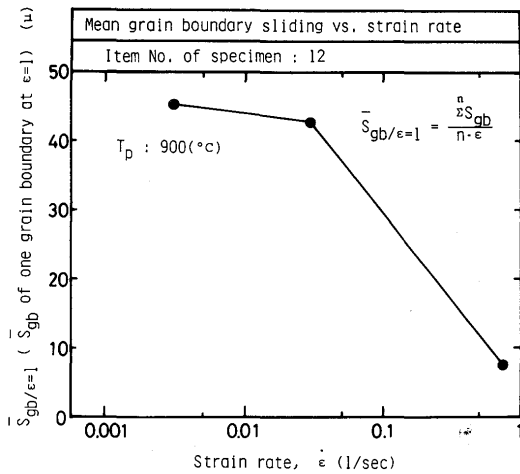
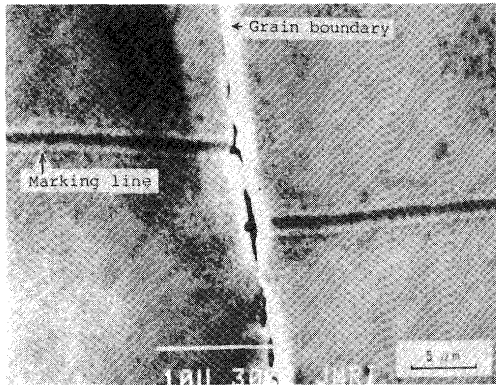
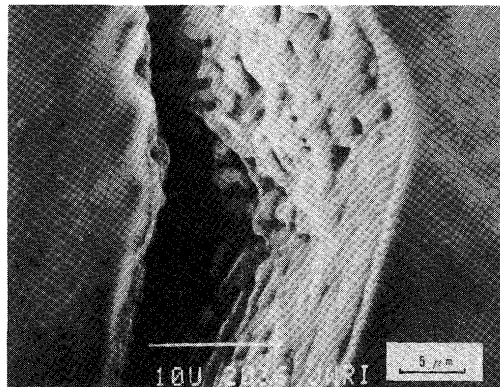


Fig. 7 Relation between strain rate and average displacement of grain-boundary sliding per one grain-boundary at  $\epsilon = 1$ , testing temperature:  $900^{\circ}\text{C}$ .



(a) cavity formation by grain-boundary sliding, Item No. 12.



(b) cracking by coalescence of cavities, Item No. 1.

Fig. 8 Example of cavity formation and its coalescence on the surface of weld metal.

was not detected in the weld metal of Fe-36%Ni alloy. The wavy feature of the cracked surface closely resemble the fracture surface in the embrittlement between about  $800$  and  $900^{\circ}\text{C}$  in Nb-bearing steel which is caused by the precipitation of Nb(C, N) on the grain-boundary<sup>6</sup>. Furthermore, it is noticed that the unit size of the wavy pattern of the cracked surface equal nearly to the size of a cavity in Fig. 8(a). Therefore, it is considered that the wavy feature of cracked surface is caused by cavity forma-

tion and not by liquation, and this problem will be discussed in detail in the next paper<sup>5</sup>).

### 3.3 Effect of grain-boundary migration

As one of the behaviors of deformation mode during the hot ductility test, also grain-boundary migration was often observed. Important characteristic at the grain-boundary which migrated largely was that the displacement of the grain-boundary sliding was very small, as pointed out according to the dynamic observation in the previous paper<sup>1</sup>). One of the example is shown in Fig. 9. The ratio of grain-boundary migration  $N_{mgb}/N_{gb} \times 100(\%)$  is shown in Fig. 10. Although 20 to 30% of grain-boundaries migrates even between  $800$  and  $900^{\circ}\text{C}$  which showed minimum ductility, 40% of grain-boundaries migrates at  $1100^{\circ}\text{C}$  which showed clear tendency of recover in ductility. One of the reason why the frequency of  $S_{gb} = 0$  increases at  $1100^{\circ}\text{C}$  in Fig. 4 and  $\bar{S}_{gb/\epsilon=1}$  decreases at  $1100^{\circ}\text{C}$  in Fig. 5 is this active grain-boundary migration. Therefore, it is concluded that grain-boundary migration has a role in recovery of hot ductility by relaxation of strain concentration to grain-boundary. Similar role is also pointed out in Al-Mg alloy<sup>7</sup>).

### 3.4 Effect of dynamic recrystallization

The results mentioned above agree well with those obtained in the dynamic observation by means of hot

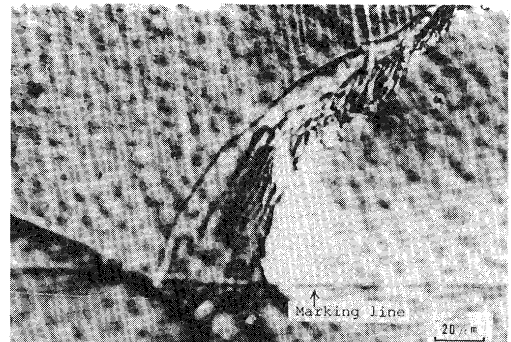


Fig. 9 Effect of grain-boundary migration on grain-boundary sliding,  $900^{\circ}\text{C}$ , C.H.S.:  $d_m$ , Item No. 12.

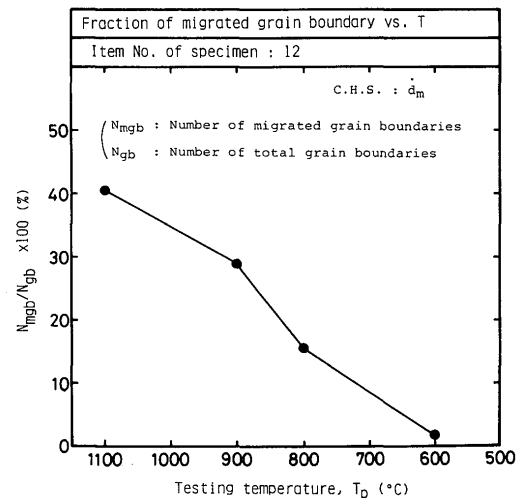


Fig. 10 Relation between temperature and ratio of grain-boundary migration  $N_{mgb}/N_{gb}$ .

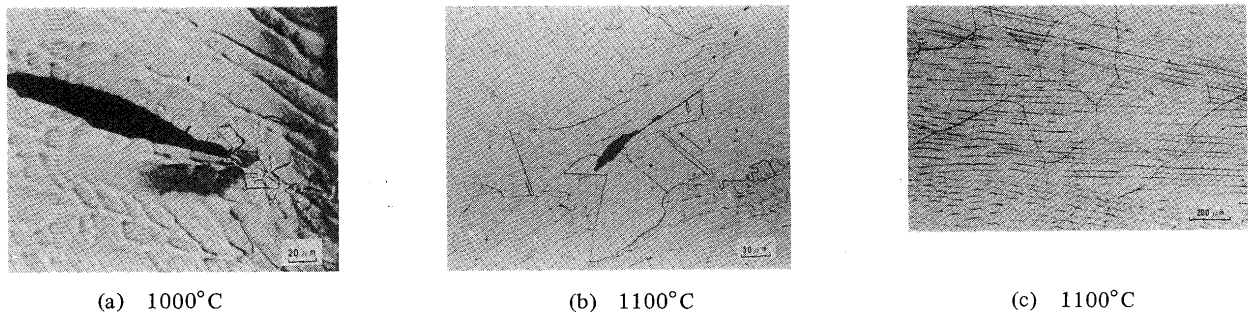


Fig. 11 Examples of dynamic recrystallization (C.H.S.:  $d_m$ ), Item No. 12.

stage microscope<sup>1</sup>). The dynamic observation, however, was not done above 880°C because of the capacity of heater. According to the literatures concerning the embrittlement in elevated temperature, dynamic recrystallization is often proposed as an improving factor of hot ductility<sup>6,8</sup>). Its experimental evidences, however, are not enough, and moreover the recrystallization largely depends on chemical composition and grain size as well known.

Examples of dynamic recrystallization are shown in Fig. 11. The dynamic recrystallization at 1000°C occurred at the tip of a crack as shown in Fig. 11(a). The dynamic recrystallization at 1100°C occurred not only around crack as seen in Fig. 11(b), but also at sites irrespective of crack as seen in Fig. 11(c). It is understood that the crack propagation is arrested in (a) and (b), and that the crack initiation itself is suppressed in (c) because of the disappearance of grain-boundary strained. Well, it may be suspected that the dynamic recrystallization occurred during the cooling after testing. In order to deny this possibility, a specimen tested at 1100°C was water-quenched in the middle of testing. Its microstructure near crack tip is shown in Fig. 12, confirming that dynamic recrystallization occurred before the fracture. Therefore, it is concluded that the dynamic recrystallization has a role in suppression of both crack initiation and propagation. The fraction of the dynamic recrystallization area  $f_R$

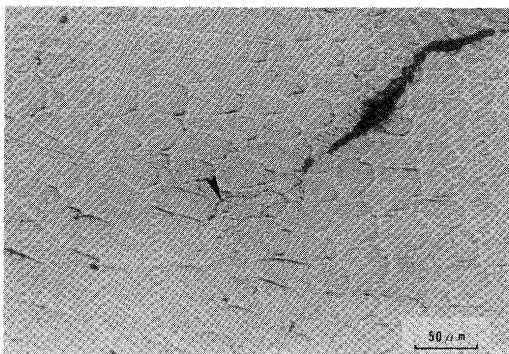


Fig. 12 Evidence of dynamic recrystallization, confirmed by water-quench in the middle of testing at 1100°C, Item No. 12. (Arrow shows the dynamically recrystallized grain.)

is shown in Fig. 13. The dynamic recrystallization did not occur up to 900°C, and then gradually increased. Another reason for the decrease in the grain-boundary sliding in Figs. 4 and 5 is the dynamic recrystallization.

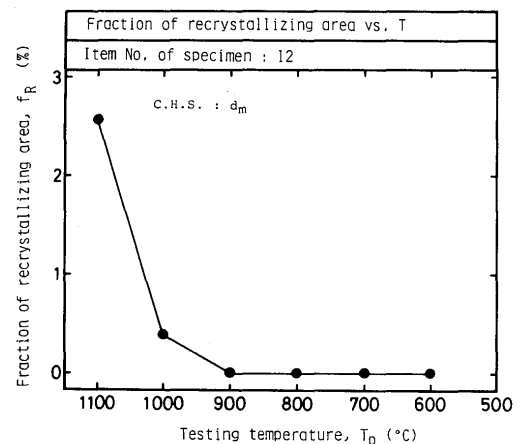


Fig. 13 Relation between temperature and fraction of dynamic recrystallization area on the surface of weld metal.

### 3.5 Effect of flow stress

It is said<sup>7</sup>) that flow stress plays an important role in imposing tensile stress against grain-boundary to make cavities. The temperature dependency of the maximum stress as the index of flow stress during the hot ductility test is shown in Fig. 14. Because the maximum stress

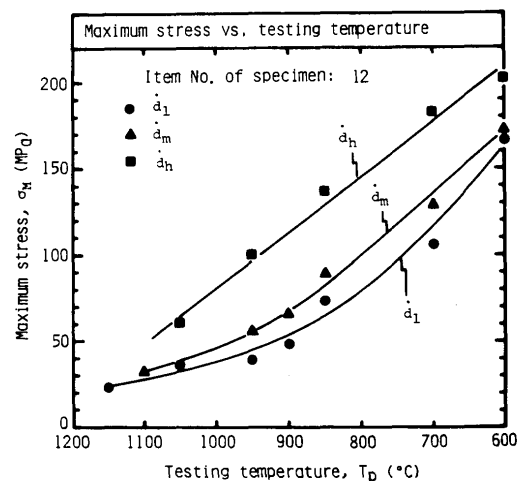
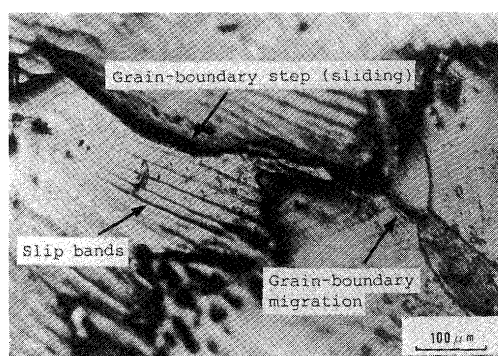


Fig. 14 Maximum stress during testing vs. temperature, indicating temperature dependency of flow stress.

decreased with the increase in temperature, it is considered that the low flow stress above about 1100°C is one of the reason for the recovery in ductility.

### 3.6 Grain-boundary sliding and cavity formation in actual weld cracking process

Examples of the surface of weld metal after the cracking test are shown in Fig. 15. It is observed in Fig. 15(a) that the level of the surface is different depending on grains, and this means that there occurred grain-boundary step, namely grain-boundary sliding. Also slip bands and grain-boundary migration can be seen. In Fig. 15(b) cavities and their coalescence are observed, and these size is nearly similar to that in Fig. 8(a) in the simulated hot ductility test. Therefore, it is understood that the hot ductility test simulated well the microstructural behaviors in actual weld cracking process.



(a) grain-boundary sliding, grain-boundary migration and slip bands, Item No. 13.



(b) formation and coalescence of cavities, Item No. 10.

Fig. 15 Microstructural deformation modes and cavity formation in actual weld cracking test.

ility test simulated well the microstructural behaviors in actual weld cracking process.

### 4. Conclusions

Main conclusions obtained are as follows.

- 1) Grain-boundary sliding is remarkable at about 900°C where hot ductility showed the minimum value. Crystal slip bands within grains instead of grain-boundary sliding is conspicuous at 600°C where hot ductility had a clear tendency to recover. Grain-boundary sliding is relieved by grain-boundary migration and dynamic recrystallization together with the decrease in flow stress at 1100°C where the hot ductility also had a tendency to recover.
- 2) Grain-boundary sliding is reduced by the increase in crosshead speed, and this explains well the dependency of the hot ductility on the crosshead speed.
- 3) Grain-boundary sliding causes cavity formation and its coalescence, which precede the reheat hot cracking.
- 4) According to the results in the above, it is concluded that grain-boundary sliding and its resultant cavity formation are prerequisite to the reheat cracking in the weld metal of Invar.

### Acknowledgement

The authors would like to thank Kawasaki Steel Corp. for the offering of materials used.

### References

- 1) Y-C. Zhang, et al.: Trans. JWRI, 14 (1985), p. 313.
- 2) Y-C. Zhang, et al.: Trans. JWRI, 14 (1985), p.107.
- 3) F. Matsuda, et al.: Trans. JWRI, 13 (1984), p.241.
- 4) F. Matsuda, et al.: to be published.
- 5) Y-C Zhang, et al.: Trans. JWRI, 14 (1985), p. 325.
- 6) C. Ouchi and K. Matsumoto: Trans. ISIJ, 22 (1982), p. 181.
- 7) M. Otsuka and R. Horiuchi: J. Japan Inst. Met., 48 (1984), p.1143 (in Japanese).
- 8) M. Ohmori, et al.: J. Japan Inst. Met., 47 (1983), p.775 (in Japanese).